PRAMANA
— journal of
physics



Vol. 59, No. 1
July 2002
pp. 113–131

# Fabrication of polystyrene hollow microspheres as laser fusion targets by optimized density-matched emulsion technique and characterization

K K MISHRA, R K KHARDEKAR, RASHMI SINGH and H C PANT
Centre for Advanced Technology (CAT), Indore 452 013, India

MS received 26 June 2001; revised 7 December 2001

**Abstract.** Inertial confinement fusion, frequently referred to as ICF, inertial fusion, or laser fusion, is a means of producing energy by imploding small hollow microspheres containing thermonuclear fusion fuel. Polymer microspheres, which are used as fuel containers, can be produced by solution-based micro-encapsulation technique better known as *density-matched emulsion technique.* The specifications of these microspheres are very rigorous, and various aspects of the emulsion hydrodynamics associated with their production are important in controlling the final product. This paper describes about the optimization of various parameters associated with density-matched emulsion method in order to improve the surface smoothness, wall thickness uniformity and sphericity of hollow polymer microspheres. These polymer microshells have been successfully fabricated in our lab, with 3–30 $\mu$m wall thickness and 50–1600 $\mu$m diameters. The sphericity and wall thickness uniformity are better than 99%. Elimination of vacuoles and high yield rate has been achieved by adopting the step-wise heating of $W_1/O/W_2$ emulsion for solvent removal.

**Keywords.** ICF target design; multiple emulsions; SEM; AFM.

**PACS Nos 52.27.Bc; 52.57.Fg; 82.70.Kj; 83.80.Iz**

## 1. Introduction

Inertial confinement fusion (ICF), is an approach to controlled fusion that depends on rapid heating and compression of fusion fuel contained in a spherical target (such as a polymer or a glass shell) of several millimeter diameters to ultra high densities (1000 times liquid density $\sim$200 g/cm$^3$), by high power driver beams. At these densities, and temperature around 10 KeV, the fusion reaction rate is high enough to allow efficient burning before the plasma disassembles.

ICF requires high-quality hollow microsphere as fuel container. These targets need to be fabricated with very smooth surfaces (of the order of 10 nm) and high order of wall thickness uniformity and sphericity (better than 99%) [1]. Glass microspheres conventionally have fulfilled most of the above-mentioned requirements, including high tensile strength and low permeability for hydrogen isotopes filled at high pressures (50–150 atm). Glass microspheres, however, consists of high-$Z$ material emitting undesirable hot electrons and

X-rays that preheat the fuel, resulting in poor compression. Preheating problem became a strong impediment to achieve high compression ($\sim 10^3$ X). Polymer shells were preferred as an alternative to glass microspheres. Being a low-$Z$ material, polymer shells are mostly free from preheating problems and have emerged as good alternative to glass microspheres. Although polymer shells have lower retentivity and tensile strength than that of glass, these parameters can be improved by providing various overcoats.

An intense development programme has been undertaken in Targets Lab, Centre For Advanced Technology, Indore, to develop polymer shells with desired parameters, as mentioned above and development of overcoats necessary to improve the retentivity and tensile strength to bring polymer microspheres at par with glass microsphere.

## 2. Major constraints in target design

### 2.1 *Rayleigh–Taylor instability* [2–5]

As mentioned above, the targets used for ICF must meet very stringent criteria for dimensional uniformity. The diameter and wall thickness of the microsphere must be controlled within a few percent, but the most precise tolerances are on the sphericity of the sphere, the thickness uniformity, and surface smoothness.

Degradation from spherical symmetry during the implosion limits the achievable compression ratios and could quench the ignition. The main source of such asymmetry is hydrodynamic instability (such as Rayleigh–Taylor (R–T) instability) seeded by spherical asymmetry and surface non-uniformity of the fuel container (hollow microsphere). Any surface non-uniformity even of the order of 10 nm or more can induce the R–T instability at the contact surface between the high density shell accelerated inwardly and lower density plasma corona at ablation front. The instability grows more rapidly for large density differences at shell interfaces, for large accelerations and for short wavelengths disturbances. Most serious instabilities are those that occur at wavelength comparable to the shell thickness. The amplitude of the R–T growth is given as

$$A(t) = A_0 \exp(\gamma t) \tag{1}$$

where $A_0$ is the initial perturbation amplitude. In classical analysis, for the simple case of a heavy fluid of density $\rho_2$ supported above a lower density fluid of density $\rho_1$, the growth rate of R–T instability is given by

$$\gamma = \sqrt{\alpha_{\mathrm{A}} kg} \tag{2}$$

where $\alpha_{\mathrm{A}}$ is the Atwood number given by $(\rho_2 - \rho_1)/(\rho_2 + \rho_1)$, $k$ the wave number or mode number, and $g$ the acceleration due to gravity.

At the ablation front, however, the classical growth rate will be modified by ablative stabilization. With a variety of simulation results, the formula for R–T instability growth rate in laser–plasma interaction is given by

$$\gamma = \alpha_{\mathrm{RT}} \sqrt{\frac{kg}{(1 + kL_{\mathrm{m}})}} - \beta k V_{\mathrm{a}} \tag{3}$$

where $\alpha_{RT} = 0.9, \beta =$ 3-4, and $V_a$ is the mass ablation velocity at the ablation front which is related to mass ablation rate as

$$V_a = \dot{M}/\rho_0$$

with $\rho_0$ being the peak density at the ablation front and $L_m$ is the minimum density-gradient scale length. This mechanism of stabilization is called ablative stabilization.

Figure 1 plots the classical number of R–T e-folds and the value of the same with ablative stabilization vs. the mode number. It is obvious from the figure that maximum growth for R–T instability is near mode number 100. So extra care is required for these modes during targets fabrication. R–T instability can also limit the allowable aspect ratio $(R/\Delta R)$ of the target shells, because very thin-walled targets are more susceptible to the instability.

### 2.2 *Fuel preheat* [6,7]

The work that is needed to compress the D-T fuel depends on the isentrope along which the compression occurs. If the fuel is initially preheated by some mechanism (such as hot electrons or photons generated by the driver beam deposition in the outer layers of the target or premature shocking by an unshaped driver pulse), then more work is required to reach the same final pressure. To avoid this problem the fuel must be shielded from these hot particles.

## 3. Emulsions [8]

Emulsions are colloidal solutions in which the dispersed phase and the dispersion medium are both fluids. When oil is dispersed in aqueous medium, two distinct types of emulsions may be formed: a dispersion of fine oil droplets in an aqueous medium known as oil-in-

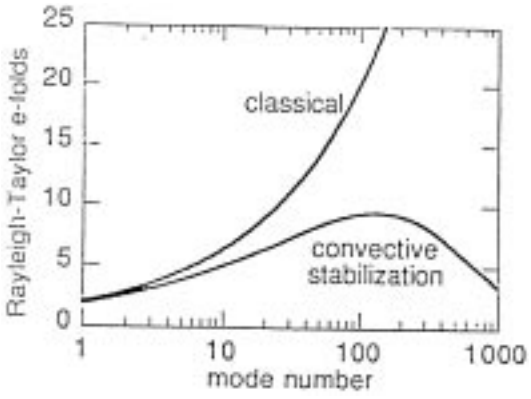


**Figure 1.** Typical number of exponentiations of the ablative Rayleigh–Taylor instability during an implosion. The upper classical curve assumes a growth rate proportional to square root of *ka*. The lower curve includes ablative (convective) stabilization. The maximum growth is near 100.

water (O/W) emulsion or of aqueous droplets in oil known as water-in-oil (W/O) emulsion. In some special cases a bicontinuous emulsion may be formed in which one phase forms a continuous network in the other. Whether W/O or O/W emulsion will be formed or not, depends on a number of factors. If the ratio of the amount of two phases (the ratio of phase volumes) is very low, the phase presents in lower volume is often the disperse phase; if the phase volumes are roughly equal, other factors determine which type of emulsion will be formed.

In the presence of surfactant, a surfactant film separating oil and water prefer to curve towards the oil to form the oil drops in water or towards the water to form water drops in oil. This dependency can be quantified in terms of *surfactant number* $N_s$. Surfactant number $N_s$ for a dilute solution of a surfactant is given by

$$N_s = v/la_0 \tag{4}$$

where $v$ stands for the volume of hydrophobic portion of the surfactant molecule, $l$ is the length of the hydrocarbon chains and $a_0$ is the effective area per head group. For $N_s < 1$ the surfactant prefers curvature towards oil, while for $N_s > 1$ it prefers to curve towards water. Only for special case $N_s = 1$ film remains planar at the interface. Schemes of W/O and O/W emulsions are shown in figure 2.

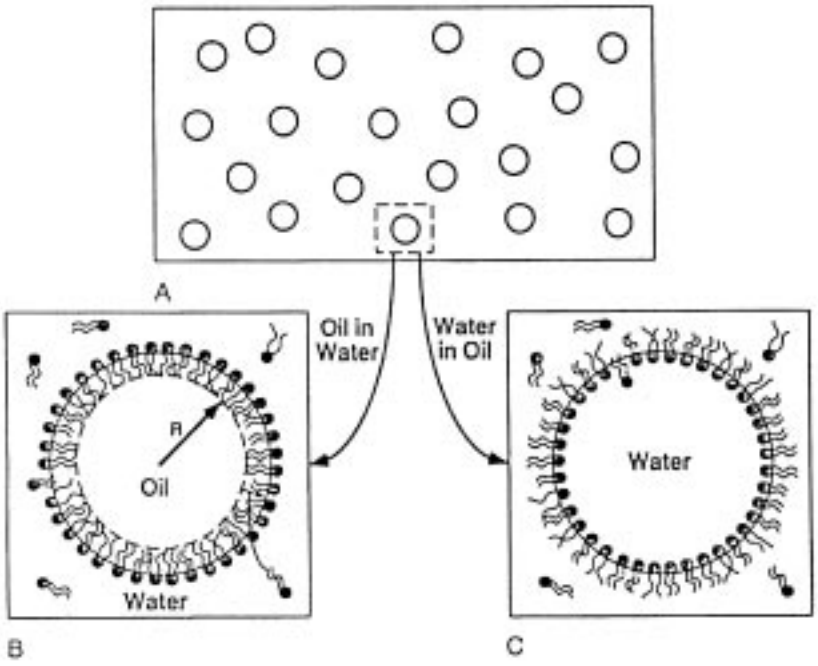


**Figure 2.** (**A**) Droplet emulsion phase, (**B**) oil-in-water (O/W), (**C**) water-in-oil (W/O) type.

### 3.1 *Multiple emulsions* [9,10]

Multiple emulsions are very complex systems and are composed of droplets of one liquid dispersed in larger droplets of a second liquid, which is surrounded by continuous phase. Typically the internal droplet phase will be miscible with or identical to the final continuous phase. Such systems may be W/O/W emulsions, where internal and external phases are aqueous, or O/W/O, which have the reverse composition. Multiple emulsions involve various phases and interfaces and so they are inherently unstable, even more than conventional 'simple' emulsions. Their surfactant requirements are such that two stabilizing systems must be employed: one for each oil–water interface. Each surfactant or mixture must be optimized for the type of emulsion being prepared but must not interfere with the companion system designed for the opposite interface. Long-term stability, therefore, requires careful consideration of the characteristics of the various phases and surfactant solubilities.

Preparation of multiple emulsion requires very judicious choice of surfactant or surfactant combinations to produce a system that has useful characteristics of formation and stability. A general procedure for the preparation of a $W_1/O/W_2$ multiple emulsion involves the formation of a primary emulsion of water-in-oil using a surfactant suitable for the stabilization of $W_1/O$ system. Primary emulsion is then emulsified in a second aqueous solution containing a second surfactant system appropriate for the stabilization of the secondary $W_1/O/W_2$ emulsion. As discussed above, because of the possible instability of the primary emulsion, great care must be taken in the choice of secondary dispersion method. The nature of the droplets in a multiple emulsion depends on the size and stability of the primary emulsion.

### 3.2 *Stabilization of emulsions*

The formation of an emulsion, which involves an increase of interfacial area between the two phases, is accompanied by an increase in free energy. Thus an emulsion represents a state of higher free energy than that corresponding to the material in bulk; passage to a state of lower free energy will therefore tend to occur spontaneously unless there is a substantial energy barrier preventing the elimination of emulsion state. In the presence of such a barrier the system will be *metastable* and may remain in that state for a very long time (figure 3a). Conversely if the conditions are adjusted so that the energy barrier becomes negligibly small, or disappears altogether (figure 3b and 3c), then the emulsion becomes *unstable*. Thus preparation and stabilization of emulsion systems is closely tied up with the factors that give rise to free-energy barriers of adequate height to prevent the breakdown of the emulsion state. In the case of emulsion systems the energy necessary to carry a system over the energy barrier comes from the Brownian motion of the droplets.

In practice, the barrier height is found to be a sensitive function of several factors including the composition of the medium, temperature and pressure. Instability and flocculation are, therefore, more often caused by the reduction in the height of barrier resulting from a change in one or more of these factors.

A situation peculiar to an emulsion system is that in which the free energy curve has the form shown in figure 3d. Here aggregation is prevented by a high-energy barrier, but preceding this is a relatively shallow minimum called a secondary minimum to distinguish

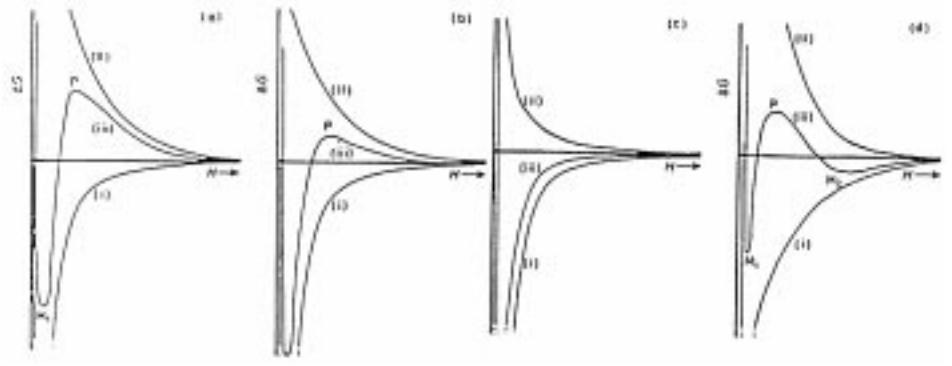

**Figure 3.** Some possible forms of total-interaction free energy (iii) resulting from a combination of attractive (i) and repulsive (ii) contributions.

it from the deep primary minimum. If the depth of the secondary minimum is of the order of a few $kT$, then a small relatively weakly bound aggregates (flocs) can form. These have limited lifetime, and a kinetic equilibrium may be set up between single particles and flocs, which is often described as week flocculation or secondary minimum flocculation. An important feature of such a situation is that, although the flocs are sufficiently stable not to be completely dissociated by Brownian motion, they may disintegrate under externally applied hydrodynamic forces, such as vigorous stirring.

In general there are two practical mechanisms which give rise to free energy barrier to provide stability to a colloidal system – electrostatic repulsion between electrical double layers and steric or entropic stabilization.

3.2.1 *Stabilization by electrostatic repulsion*: In emulsions surfactant ions are specifically adsorbed, leading, in the case of cationic surfactants, to a positively charged surface and, in the case of anionic surfactants, to a negatively charged surface. Thus an ionic atmosphere is developed around each charged colloidal particle (emulsion droplet) and this ionic atmosphere is known as electrical double layer. The charge on the droplet is distributed over its surface and is just balanced by the total charge in the double layer in which there is an excess of oppositely charged ions (counter ions). As two charged surfaces come together, the double layers overlap and as a rough approximation the electrical potential arising from the two surfaces are additive. The electrical potential between the surfaces thus increases. This increase implies an increase in the electrical contribution to the free energy of the system. The consequent repulsive energy arising from the double layer overlap is also exponentially dependent on the separation $H$. The approximate equation for two parallel plates per unit area is

$$\Delta G^{\text{electrostatic}} = \left(\frac{64c^0kT}{\kappa}\right) \exp(-\kappa H), \tag{5}$$

where $c^0$ is the concentration of ions at the reference level taken as the zero of energy $(\varphi = 0)$ and $T$ is the temperature. When the Van der Waals attractive potential is added, the total potential energy for this interaction between two parallel surfaces takes the form

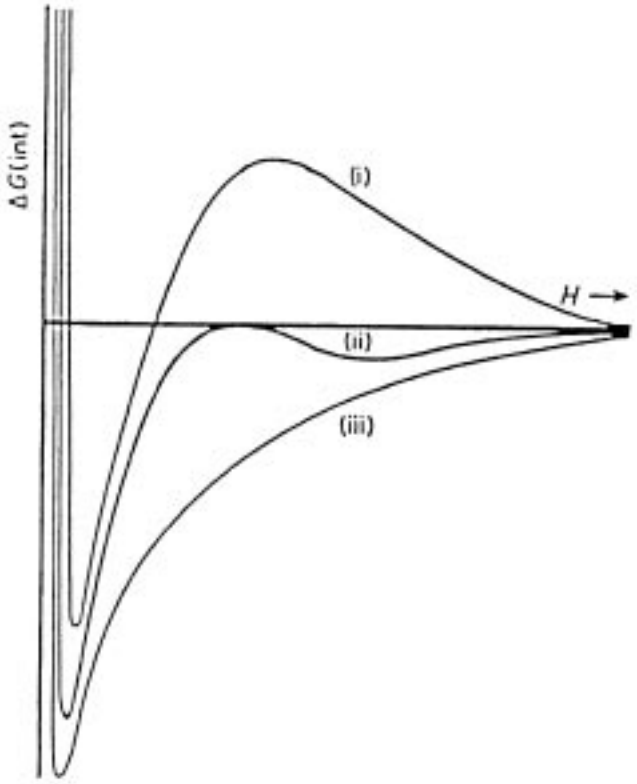


**Figure 4.** Total interaction free energy for elctrostatically stabilized colloidal sytem.

$$\Delta G^{\text{total}} = \left(\frac{64c^0kT}{\kappa}\right) \exp(-\kappa H) - \frac{A_H}{12\pi H^2}. \tag{6}$$

This interaction will develop steadily as they approach. The resulting repulsion between the droplets may be interpreted as that the two ionic charged clouds, of the same sign, repel one another in much the same way as the electron clouds around atoms and molecules. Total interaction energy curves for different electrolyte concentrations are shown in figure 4. Curves (i), (ii) and (iii) refer to increasing electrolyte concentration.

3.2.2 *Stabilization by steric or entropic repulsion*: If two colloidal particles have an adsorbed layer of a polymeric surfactant, as they approach each other, these layers begin to interpenetrate. Such interpenetration can have two effects: an osmotic effect due to increase in the local concentration of the adsorbed species between the two particles and an entropic or volume restriction effect because the interacting species begin to loose certain degrees of freedom due to crowding. In both cases, the local system will experience a decrease in entropy, which will of course, be unfavorable, while the osmotic effect may be accompanied by an unfavorable enthalpic effect due to desolution of more closely packed units. In order to regain the lost entropy, the particles must move apart allowing them

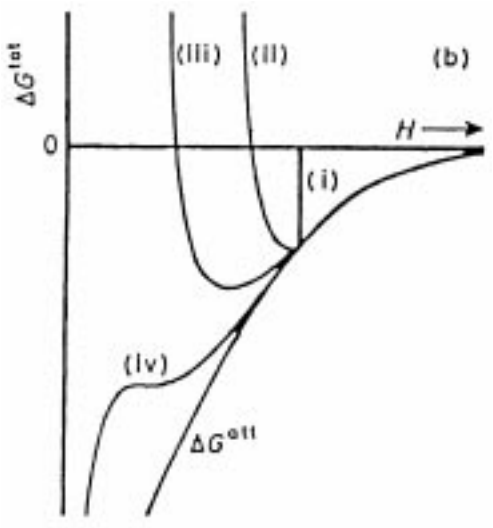


**Figure 5.** Total interaction free energy curves for sterically stabilized colloidal systems.

more freedom of movement, while solvents move in to resolvate the units. The result is an energy barrier retarding the approach of particles and provide an effective mechanism for stabilization. This mechanism of stabilization using polymeric surfactant is known as steric stabilization. In the pure sterically stabilized system, the net energy of interaction will be the sum of the attractive vander Waals forces and the repulsive steric interactions

$$\Delta G^{\text{total}} = \Delta G^{\text{steric}} - \Delta G^{\text{att}} = T\Delta S - \frac{A_H}{12\pi H^2}. \tag{7}$$

Total interaction free energy curves for sterically stabilized colloidal system are given in figure 5. Curve (i) is for densely packed adsorbed layer on hard surface and curves (ii)–(iv) are for decreasing density of the adsorbed layer, at constant adsorbed layer thickness.

## 4. Experimental process

The *density-matched emulsion method* was originally developed by Kubo and coworkers at ILE Osaka, Japan [11,12]. We have further optimized this method to produce vacuole-free high aspect ratio polymer microspheres. In density-matched emulsion technique, a water phase is emulsified in an organic solution of desired polymer. This primary emulsion of water/oil ($W_1$/O) type is dispersed into a second water phase yielding a water/oil/water ($W_1$/O/$W_2$) type multiple emulsion. Here sodium lauryl sulfate is used as primary surfactant to form $W_1$/O emulsion and polyvinyl alcohol (PVA) acts as secondary surfactant in the formation of multiple emulsion ($W_1$/O/$W_2$). The oil phase solvent is removed thermally in water referred to as under water drying, leaving polymer shells that contain water. Hollow microsphere is then obtained by slow drying of water. Schematic diagram of the process is given in figure 6. Complete process consists of the following steps:

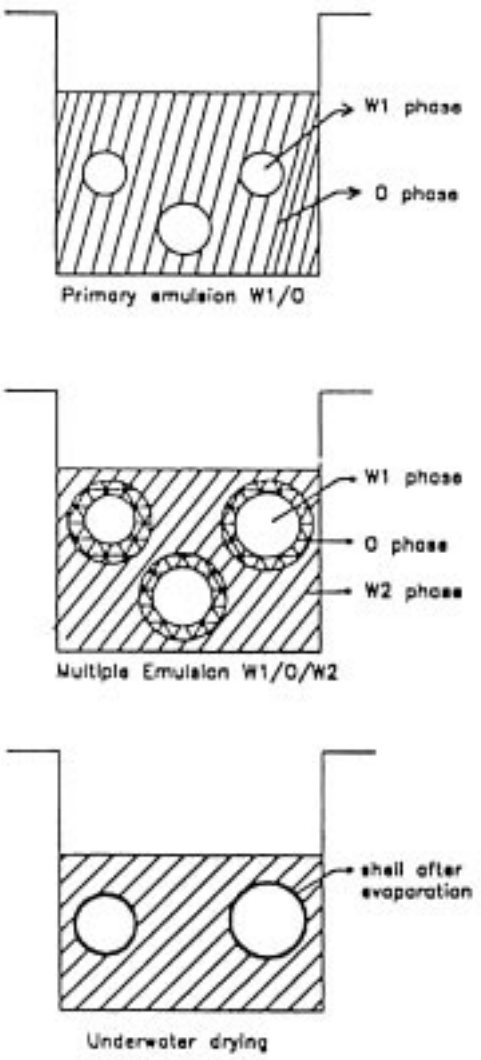


**Figure 6.** Schematic diagram of density-matched emulsion technique.

*Step* 1. *Preparation of oil phase, $W_1$ phase and $W_2$ phase*: We have used polystyrene to prepare oil phase (O-phase). Equivalent mixture of 1-2 dichloroethane and benzene has been used as solvent. These solvents are selected because both of them have almost the same boiling temperature, temperature dependence of vapor pressure and heat of vaporization, which help in preventing change in density during drying process. We varied the concentration of oil phase from 2 wt% to 8 wt% and filtered the solution through teflon filter having a pore size of 0.2 $\mu$m.

Water phase $W_1$ was prepared by adding surfactant (sodium lauryl sulfate) in water. The concentration of $W_1$ phase was varied from 0.1 wt% to 1.0 wt%.

Water phase $W_2$ was prepared by adding polyvinyl alcohol (PVA) in water. The concentration of $W_2$ phase was varied from 2 wt% to 5 wt%.

*Step* 2. *Preparation of $W_1/O$ emulsion*: 5ml $W_1$ phase was mixed in 10 ml of oil phase and the mixture was shaken manually until homogeneous $W_1/O$ emulsion is formed. In the formation of this primary emulsion, surfactant (sodium lauryl sulfate) plays a very important role.

*Step* 3. *Preparation of $W_1/O/W_2$ emulsion*: $W_1/O$ emulsion prepared in step 2 was poured in a beaker filled with $W_2$ phase (500 ml). The emulsion was stirred with a magnetic rotator initially at 400 rpm for 15 s to sufficiently disperse the $W_1/O$ emulsion into $W_1/O/W_2$, and then rotational speed was reduced to 150 rpm to avoid agglomeration of emulsion drops. This $W_1/O/W_2$ emulsion was kept in a water bath having temperature around 60°C.

*Step* 4. *Drying of $W_1/O/W_2$ emulsion droplets*: In order to remove the oil phase solvent, the $W_1/O/W_2$ emulsion was heated. Temperature of the water bath was varied from 60°C in steps of 5°C after every 2 h, and finally the temperature was raised to 80°C. Polystyrene microspheres were washed with distilled water to remove PVA and were immersed in ethyl alcohol (ethanol) for 48 h to replace $W_1$ phase trapped within the microsphere with ethanol. Ethanol helped to smooth the defects on the inner surface of the microsphere. Subsequently these polystyrene microshells were kept in air for the next 48 h to evaporate ethanol.

## 5. Results and discussions

Very good quality polymer microspheres are produced, having surface smoothness of the order of 10 nm, sphericity within 1% and wall thickness uniformity within 1%. The wall thickness of the microsphere is proportional to the concentration of polystyrene in oil phase. The concentration of the oil phase was varied from 2% to 9% and wall thickness was estimated by observing the cross-section. Microspheres were broken by a sharp knife to produce clear cross-section of the wall. Relation between oil-phase wt% and wall thickness is plotted in figure 7.

The lower limit of the diameter of the microsphere is due to breaking of the emulsion droplet during drying process and because of density mis-matching and the upper limit of microsphere is mainly determined by rotational speed of the magnetic stirrer.

Control of vacuoles in the emulsion technique is very troublesome and very important from the viewpoint of hydrodynamic instabilities. The degree of vacuoles generation depends on the molecular weight of polystyrene mixing ratio of the solvent, dust in the solution, gases dissolved in the solvent and temperature history of the drying process. We have been able to reduce the number of vacuole in the shells using 0.2 $\mu$m pore size teflon filter and step-wise heating of the $W_1/O/W_2$ emulsion during drying process.

### 5.1 *Variation in conventional method*

We have introduced certain variation in conventional density-matched emulsion method to optimize the method for high yield rate. A magnetic rotor, which is an octagonal bar of

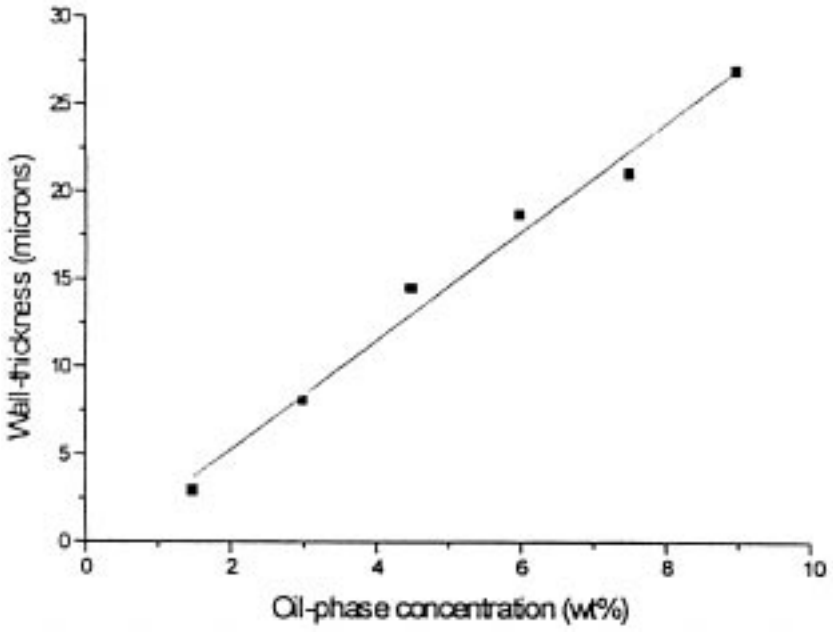


**Figure 7.** Relationship between wall thickness of the microsphere and oil-phase concentration.

length 25 mm, was used to stir $W_1/O/W_2$ emulsion. This small size magnetic rotor in the shape of octagonal bar has very low probability of striking emulsion droplets, as compared to conventionally used vertical fin-type rotor. Thus survival rate of emulsion droplets is more in our set up.

A water bath was used to remove the solvent from $W_1/O/W_2$ emulsion. This water bath helps in maintaining uniform temperature across the height of the beaker containing the emulsion and avoids any temperature gradient, which can give rise to convection currents. During solvent removal process, temperature of the water bath was increased in steps from 60°C to 80°C, rather than increasing it abruptly to 80°C. It has been observed that yield rate as well as quality of the microspheres is improved drastically by adopting this step-wise heating. Proportion of surfactant was also optimized, by varying the concentration of $W_1$ phase from 0.1% to 1%. Very good yield was obtained with 0.4–0.5 wt% concentration.

### 5.2 *Role of density matching*

For a spherical drop of radius $R$ and effective density $\rho$ falling under gravity in a fluid of density $\sigma$, following three forces acts on the drop:

1. Weight $W$ (gravity force) of the drop acting vertically downwards through the center of gravity is given by

$$W = \frac{4}{3}\pi R^3 \sigma g. \tag{8}$$

2. Upthrust $U$ due to buoyancy is given by

$$U = \frac{4}{3}\pi R^3 \rho g. \tag{9}$$

3. Viscous drag $F$ acting upwards is given by

$$F = 6\pi\eta a v \tag{10}$$

and

$$\text{Net downward force } = W - (U - F). \tag{11}$$

This force is responsible for the downward acceleration of the spherical drop. As the velocity of the spherical drop increases, the viscous force $F$ also increases. A stage is reached when the weight of the spherical drop is just balanced by the sum of the upthrust and viscous drag. At this stage there is no resultant force on the spherical drop. Consequently drop begins to move with terminal velocity $v_0$. At this stage

$$\begin{aligned} &F = U + W, \\ &\frac{4}{3}\pi R^3(\rho - \sigma)g = 6\pi\eta a v, \\ &v = v_0 = \frac{2}{9}\,\frac{(\rho - \sigma)2Rg}{\eta}. \end{aligned} \tag{12}$$

Further, if $\rho = \sigma$ then $v_0 = 0$, and the drop will remain in rest position.

This concept of density matching is very important for fabrication of microspheres using emulsion technique. Density matching avoids any asymmetry (elongation or deformation due to gravity) in emulsion droplets and also prevents sedimentation and creaming of emulsion droplets.

Thus, ultimate sphericity of microsphere and yield both depends on how accurately densities of different phases are matched during the process.

### 5.3 *Role of surfactant in emulsion formation and stabilization*

Surface active agents (surfactants) represent a class of chemical compounds consisting of a hydrocarbon (or fluorocarbon) portion and polar ionic portion. The hydrocarbon portion, which is referred to as hydrophobic part, has a weak affinity for the water molecule in an aqueous environment. In contrast, the ionic or polar portion of molecules (referred to as hydrophilic group) has a strong affinity for the water molecules as a result of ion–dipole and dipole–dipole interaction. This hydrophilic–hydrophobic combination makes surfactants unique in their physical properties.

Surfactant plays an important role both in preparation and stabilization of the emulsion. The role of surfactants in emulsion preparation is attributed to two main effects. The first and most obvious effect is the reduction in interfacial tension $\gamma$ (the interfacial tension $\gamma_{\text{oil/water}}$, falls from 30–50 mN m$^{-1}$ to a few mN m$^{-1}$ at and above cmc of surfactant and

$\gamma_{\text{water/air}}$ falls from 72 mN m$^{-1}$ to 30 mN m$^{-1}$), and hence the work required to increase the surface tension on emulsification ($\gamma\Delta A$) or the free energy $\Delta G_{\text{em}}$ needed to disperse a liquid of volume $V$ with drop of radius $R$ ($\Delta G_{\text{em}} = \gamma \cdot 3V/R$). Pressure gradient required to split a droplet in two parts ($\Delta p/\Delta x = 2\gamma/RR$) will also be smaller due to reduction in the interfacial tension $\gamma$.

The second and the more important effect is the creation of interfacial tension gradient sometimes referred to as *Gibbs Marangoni effect* which is crucial for prevention of thinning and disruption of the liquid film between the droplets. When a film is subjected to local stretching as a result of some thickness fluctuation, the local increase in surface area is accompanied by a decrease in surface excess of adsorbed surfactant in that region and hence local increase in interfacial tension, thus opposing stretching (known as *Gibbs effect*). The *Marongoni effect* arises from the finite time required for the surfactant molecules to diffuse to the depleted region, which tends to dampen the fluctuation in the film. These surfactant films are very crucial in preventing joining off the emulsion droplets, a process normally known as coalescence. This process is most difficult to prevent in emulsion and its nature depends on the nature and concentration of the surfactant used. Sodium lauryl sulfate ($C_{12}H_{25}SO_4Na$) has been used in this process which is an anionic type ($C_{12}H_{25}SO_4{}^-Na^+$) surfactant. When two droplets with surfactant layer approach towards each other their associated double layers begins to interact and cause repulsion of emulsion droplets.

## 6. Characterization of microspheres

The targets used for ICF must meet very stringent criteria for dimension and uniformity as discussed earlier. The target defects are classified into three types. Type I defects are non-concentrecities of the inner and outer walls of a target. Type II defects are non-sphericities of inner or both walls. The Type III defects are small scale defects such as wart or dimple, on either surface, or a density variation in the coating. It is estimated that Type I or Type II smaller than 1% in $t/\mathrm{d}t$ will not degrade target performance, where $t$ is the average wall thickness and d$t$ is the variation about the average. Defects of Type III must be smaller than 0.1% in $t/\mathrm{d}t$ if they cover an area of $t^2$ [13].

Sphericity of microsphere has been measured by optical microscope in various orientations. Random samples were selected from different batches, deviation in the sphericity was not more than 1%. Picture from optical microscope are shown in figures 8 and 9. Wall thickness of polystyrene microsphere was estimated by observing the wall cross-section by scanning electron microscope. The microsphere was broken by a sharp knife.

Wall-thickness uniformity of the hollow microsphere is simply defined by

$$\left\{1 - \frac{t_{\max} - t_{\text{av}}}{t_{\text{av}}}\right\} \times 100, \tag{13}$$

where $t_{\max}$ is the maximum wall thickness and $t_{\text{av}}$ is the average wall thickness of the microsphere.

Wall thickness and non-concentricity of these microshells were also measured by optical interferometry. The probe beam was interfered with the parallel reference beam to make concentric interference pattern in the microshell image. Wall thickness $t$ is given by

$$t = \frac{x\lambda}{4(n' - 1)}, \tag{14}$$

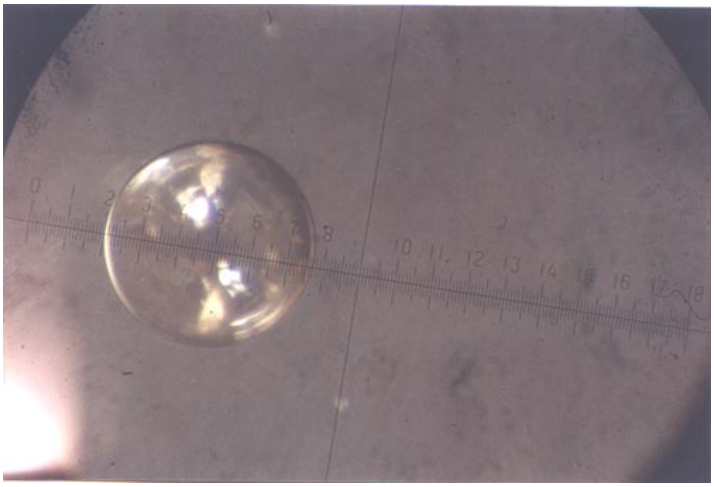

**Figure 8.** Optical micrograph of a polystyrene microsphere, diameter 1452 $\mu$m.

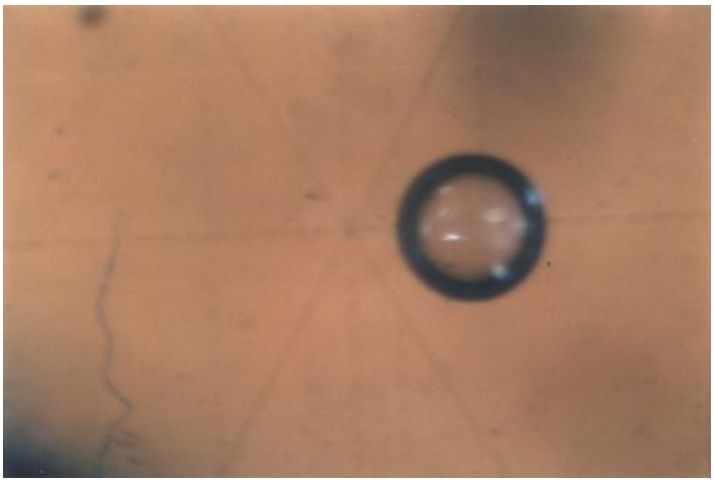

**Figure 9.** Optical micrograph of a thick-walled polystyrene microsphere, diameter 863 $\mu$m.

where $x$ is the number of fringes between the reference fringe and center of the fringe pattern on the ball, $\lambda$ the wavelength of the monochromatic source and $n'$ the refractive index of microsphere material 14]. Non-uniformity or non-concentricity of the microsphere is given by

$$\delta t = \frac{\delta r t_{\text{av}}}{r}, \tag{15}$$

where $\delta r$ is the deviation of interference pattern and microsphere center, $r$ the average radius and $t_{\text{av}}$ the average wall thickness of the microsphere. Figure 10 shows a typical interferogram of the hollow microsphere.

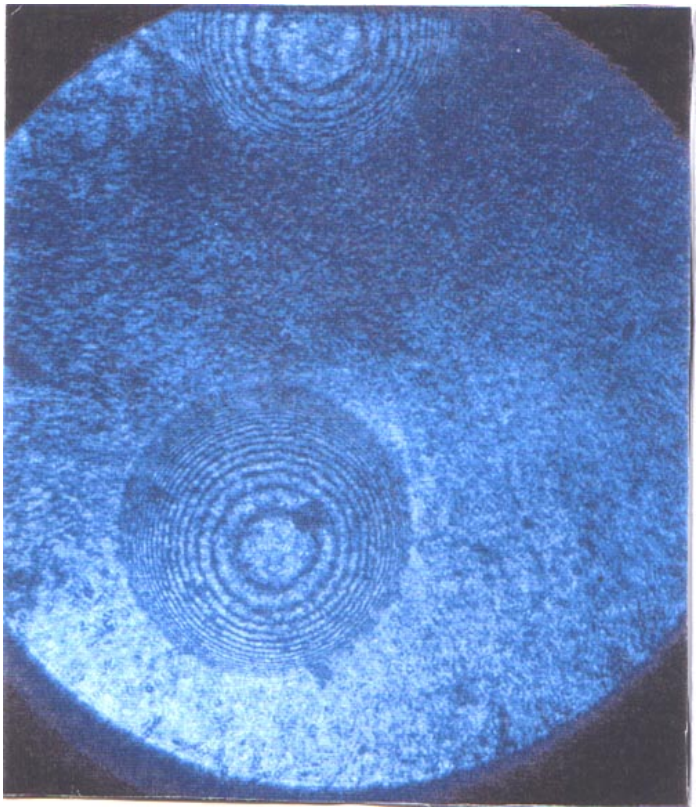

**Figure 10.** An interferogram of a microsphere showing circular fringe pattern.

Scanning electron microscope (SEM) provides higher spatial resolution than that can be achieved with optical methods. Spatial resolution of 10 nm can be easily obtained. The SEM is useful to measure the surface structure, surface contamination and internal structure of cross-sectioned samples. The polymer microspheres requires a thin conductive coating, usually of gold, to prevent image distortion due to local charging. Extensive study of microspheres and their sections was undertaken by SEM. SEM images are shown in figure 11.

The polymer microsphere were finally characterized by using atomic force microscopy (AFM). The AFM is able to image both conducting and non-conducting surfaces. The AFM has proved most useful in measuring the surface roughness of the films and microspheres in target fabrication. The AFM was performed on Digital Instrument Nanoscope at Inter University Consortium (IUC) Indore.

The nanoscope works on two resolution modes. In high-resolution mode the vertical resolution of a few nanometers is easily obtained while the scan area is restricted to 400 $\times$ 400 nm. The nanoscope being a very versatile equipment also offers low-resolution mode where large area sample can be scanned. A sample of 100 $\times$ 100 $\mu$m with vertical resolution of better than 100 nm is very convenient for a large object like the microsphere.

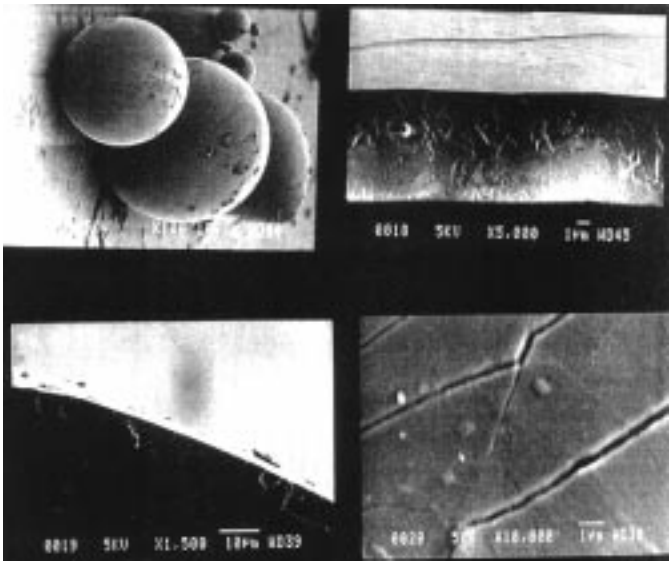

**Figure 11.** SEM images of microspheres.

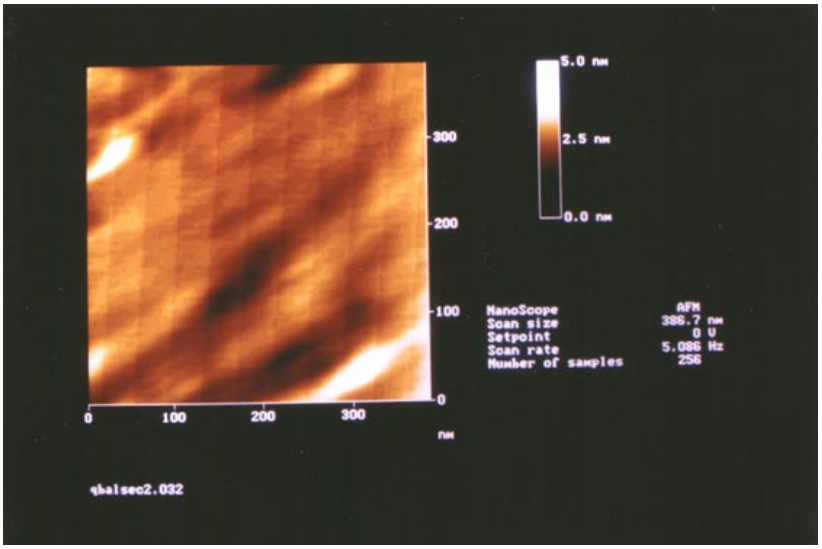


**Figure 12.** High resolution AFM scans over 400 $\times$ 400 $\mu$m area.

Figures 12 and 13 show different sections of microsphere in high-resolution modes. Figure 12 shows a typical section with 400 $\times$ 400 nm cross-sectional area. The surface is extremely smooth with variation of less than 2.5 nm rms; such smoothness of view in rms of microsphere is a very important achievement. It is the ultimate technology to the process adopted and is a measure of successful optimization of the precise parameters.

Figure 13 shows rare patches of rough granules in high-resolution mode. It should however be kept in mind that these are very small-sized features of a few tens of nm across and less than 10 nm height. A source feature of this essentially does not matter from the point of view of R–T instabilities etc. being in the admissible limits of surface roughness. Figure 14 shows the wall-section of a microsphere.

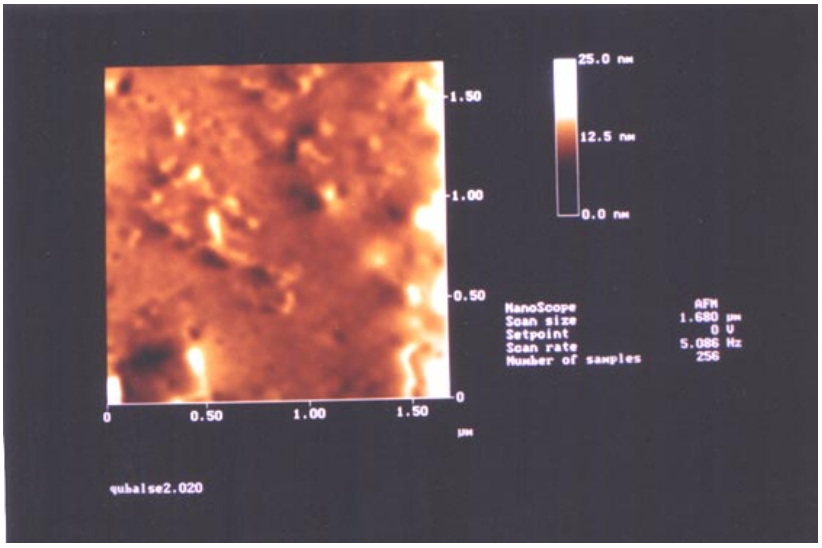


**Figure 13.** High resolution AFM scans over $1.5 \times 1.5$ $\mu$m area.

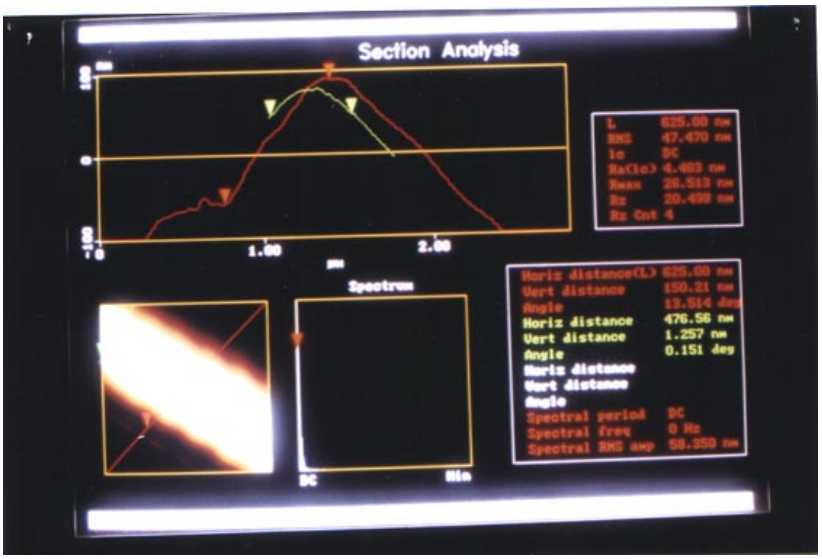


**Figure 14.** Measurement of wall thickness of PS layer of a microsphere.

## 7. Summary and conclusions

Highly spherical polystyrene hollow microspheres have been fabricated using optimized density-matched emulsion technique, with diameter and wall thickness ranging from 50 to 1600 $\mu$m and 3 to 30 $\mu$m respectively. Emulsion technique was optimized to produce vacuoles-free high aspect ratio microspheres, using step-wise heating of $W_1/O/W_2$ emulsion for solvent removal and by filtering all solutions through 0.2 $\mu$m teflon filters. The vacuoles in microsphere walls are very few and rare measuring less than 0.1 $\mu$m.

The microshells were characterized extensively using optical microscopy, scanning electron microscopy (SEM) and atomic force microscopy (AFM). The sample microshells were selected randomly from various batches. The sphericity and wall-thickness uniformity of microspheres were better than 99%, along with surface smoothness of the order of 10 nm. Large number of microspheres of sizes 50 to 100 $\mu$m were produced in every batch which are required for experiments with 1KJ high power laser facility at CAT.

Fabrication of large-sized microspheres having diameters in the range of 1000 to 1600 $\mu$m and wall thickness in the range of 3–5 $\mu$m diameter is very encouraging. These high aspect ratio microspheres generally do not survive during evaporation process at elevated temperatures. Optimization of the process by step-wise heating during evaporation resulted in the production of these high aspect ratio vacuoles-free microspheres.

Following conclusions can be drawn from the experiment:

1. The key issue to fabricate the hollow microspheres with uniform wall thickness is to equalize mass–densities of oil-phase and w-phase solution to eliminate the effect of gravity.
2. Vacuoles which are believed to result from the microphase separation of trace amount of water within the polymer/solvent wall during drying, can be reduced in number by step-wise heating of $W_1/O/W_2$ emulsion and filtering all solutions through 0.2 $\mu$m filter.
3. The number density of scratches depends on the viscosity of the $W_2$ phase, the stirring speed of the rotor and collision frequency of the microshells with the rotor.
4. Wall thickness of the hollow microsphere is proportional to the polystyrene concentration in the oil phase.
5. Double and triple shell targets can be fabricated by repeating the emulsion. For example, double shell targets can be produced from $W_1/O/W_2/O/W_3$ emulsion.

## Acknowledgements

Authors acknowledge P I John, Institute of Plasma Research (IPR), Ahemdabad, V Ganeshan, Inter University Consortium (IUC), University Campus DAVV, Indore, R V Nandedkar and Pragya Tripathi, CAT, Indore, for their contribution during the characterization of ICF targets. Finally we are thankful to D D Bhawalkar for his keen interest and valuable guidance during the work.

## References

[1] J H Campbell, J Z Granes and J F Poco, *Technol. Repts.*, Lawrence Livermore National Laboratory, Livermore, CA, Nov. (1983), UCRL 53516

[2] Modeling of Laser Imprint Inertial Confinement Fusion Targets, *LLE Review*, vol. 80
[3] S Bodner, *Phys. Rev. Lett.* **33**, 761 (1974)
[4] Leon J Radziemski and David A Cramers, *Laser induced plasma and applications* (Marcel-Dekker Inc., New York, USA, 1989)
[5] Stephen E Bodner, Denis G Colombant, John M Gardener, Robert H Lehmberg, Stephen P Obenschrin, Lee Phillips, Andrew J Schmitt and John D Sethiana, *Phys. Plasmas* **5**, 1901 (1998)
[6] J D Lindll, *Nuclear Fusion* **14**, 511 (1974)
[7] J Nuckolls, *ICF target physics overview-tropical meeting on inertial confinement fusion* (OSA, San Diego, Feb. 1980)
[8] S Voyutsky, *Colloid chemistry* (Mir Publisher, Moscow)
[9] *Surfaces, interfaces and colloids: Principles and applications* (Drew Myers, Wiley-VCH, 1999)
[10] M Satake, Y Hayashi, Y Mido, S A Iqbal and M S Sethi, *Colloidal and surface chemistry* (Discovery Publishing House, 1996)
[11] U Kubo and H Tsubakihara, *J. Vac. Sci. Technol.* **A5**, 2778 (1987)
[12] T Norimatsu, M Takagi, Y Izawa, S Nakai and C Yamanka, *J. Vac. Sci. Technol.* **A5**, 2785 (1987)
[13] R L Whitman, R H Day, R P Kurger and D M Stupin, *Appl. Opt.* **18**, 1266 (1979)
[14] B W Wienstein, *J. Appl. Phys.* **46**, 5305 (1975)